In: Monomers, Oligomers, Polymers, Composites… ISBN: 978-1-60456-877-6
Editors: R. A. Pethrick, G.E. Zaikov et al.

Chapter 7

THE SYNTHESIS AND PROPERTIES OF UNSATURATED HALOGEN -CONTAINING POLY (ARYLENE ETHER KETONE)S

A.M. Kharayev, A.K. Mikitaev, G.E. Zaikov* and R.Ch. Bazheva

Kabardino-Balkar State University,
360004, Nalchik, Chernishevskaya st. 173, KBR, Russia.
*Institute of biochemical Physics
Russian Academy of Sciences
119334 Moscow, Kosygin str., 4, Russia

ABSTRACT

Using dihydroxyl-containing olygoketones with different condensation degrees and unsaturated halogen - containing dichloroanhydrides, aromatic poly(arylene ether ketone)s (PAEK) were synthesized by means of acceptor-catalytic polycondensation. The correlation between the structure of olygoketones and properties of poly(arylene ether ketone)s were investigated. It was shown that the PAEK was characterized by a high physical and chemical properties.

Keywords: poly(arylene ether ketone), copolymerization, glass transition, dielectric properties, viscosity

INTRODUCTION

Polyethers (PEK) and polyetheretherketones (PEEK), possessing a complex of valuable properties, take an important place among thermal and heat resistant polymers; due to this some of the mentioned polymers are used in production[1-3]. Under the synthesis of PEEK the methods and conditions of synthesis play a significant role. Two approaches are noted here: the synthesis of PEEK on the basis of 4,4'-dichlorobenzophenone in high

boiling organic solvents[4] and synthesis of PEEK of block structure on the basis of 4,4'-dichlorobenzophenone by means of acceptor-catalytic polycondensation[5].

There is a great number of information in literature about the synthesis of polyetherketones on the basis of 4,4'-dichlorobenzophenone and widely known bisphenols, including 4,4'-dioxyphenyl - 2,2-propane and phenolphthalein. A great shortage of these methods is the duration of the synthesis (about 30 hours) and the high temperature (about 300^0 C and more). Besides, even in such stringent term synthesis other halogenated diphenylketones do not actively react[6-14].

In this connection, the investigation of a possibility of carrying out of a polycondensation process of getting poly(arylene ether ketone)s in greatly more soft conditions with the usage of 4,4'-dichlorobenzophenone. As 4,4'-dichlorobenzophenone in the medium of dimethylsulphoxide 150-160^0 C doesn't give with 4,4'-dioxyphenyl - 2,2-propane, and phenolphthalein polymers with high molecular weight, we used the getting block-copolyetheresterketones.

As one of monomers 1,1-bis(4-chlorophenyl)-2,2,2-trichloroethane (DDT) is chosen. A chose of this monomer is explained so that the prohibition of 1,1-bis(4-chlorophenyl)-2,2,2-trichloroethane a global scale as an insecticide faced the humanity a necessity of finding of an another application for it. As till the present day the mentioned matter is in great quantity in the storehouses and arouses a serious ecological threat to the environment, so each method of its utilization demands proper attention. The getting of different monomers from 1,1-bis(4-chlorophenyl)-2,2,2-trichloroethane for their further usage as monomers in the process of synthesis of fire-resistant polyesters is highly perspective in this regard.

With this aim 2,2-bis(4-chlorophenyl)-1,1-dichloroethylene had been got from 1,1,1-bis(4-chlorophenyl)-2,2,2-trichloroethane, and then it was used for synthesis of 4,4'-dichlorobenzophenone.

As acid component dichloroanhydride 1,1-dichloro-2,2di-(4-carboxyphenyl)ethylene was used. The leading in the structure of polymers of $>C=CCI_2$ group promotes an increase of refractoriness in conditions of preservation of high importance of mechanical properties.

EXPERIMENTAL PROCEDURE

In the present paper, poly(arylene ether ketone)s were synthesized in two steps on account of low activity of 4,4'-dichlorobenzophenone in polycondensation process and also having a desire to hold the process of synthesis under softer conditions. PAEKs were synthesized by means of acceptor-catalytic polycondensation from olygoketones (OK) on the basis of 4,4'-dioxyphenyl - 2,2-propane, containing two hydroxyl end groups and dichloroanhydride 1,1-dichloro-2,2di-(4-carboxyphenyl)ethylene. Olygoketones with different condensation degrees were synthesized by means of interaction of disodium salt of 4,4'-dioxydiphenyl-2,2-propane with 4,4'- dichlorobenzophenone in anhydrous dimethylsulphoxide (DMSO) according to the known method [14], where n=l,5,10 and 20 *(scheme 1).*

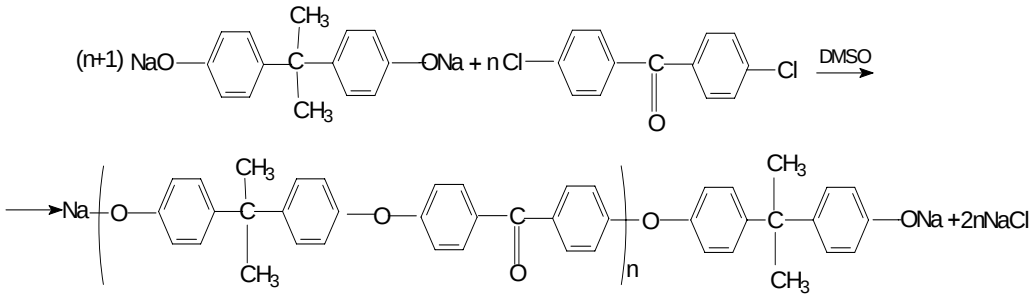

Scheme 1.

4,4'- dichlorobenzophenone was obtained from 1,1-bis(4-chlorophenyl)-2,2,2-trichloroethane (DDT) in two steps: in the first stage 2,2-bis(4-chlorophenyl)-1,1-dichloroethylene was synthesized from DDT by means of dehydrochloration; in the second stage, this product was reacted with oxide of six-valent chromium in ice acetic acid and 4,4'-dichlorobenzophenone with a melting temperature of 146°C was obtained. The given process was described by Yanota et al[15].

Some properties of olygoketones are given in table 1.

Table 1. The properties of olygoketones

Olygoketones	Condensation degree	Softening temperature(C)	Molecular weight (in carbon units)	OH-group content (%)	
				Calculated	Measured
OK-1D	1	129-132	647,78	5,36	5,30
OK-5D	5	147-152	2260,72	1,50	1,35
OK-10D	10	160-165	4293,17	0,79	0,75
OK-20D	20	167-175	8358,43	0,41	0,40

Dichloroanhydride 1,1-dichloro-2,2di-(4-carboxyphenyl)ethylene was obtained according to the *scheme 2*:

Poly(arylene ether ketone)s was obtained by the technique of acceptor-catalytic polycondensation in 1,2-dichloroethane for 1 hour at 20°C. Triethylamine was used as an acceptor-catalyser, and isopropanol - as a precipitator. The synthesized PAEK possesses the following structure (*Scheme 3):*

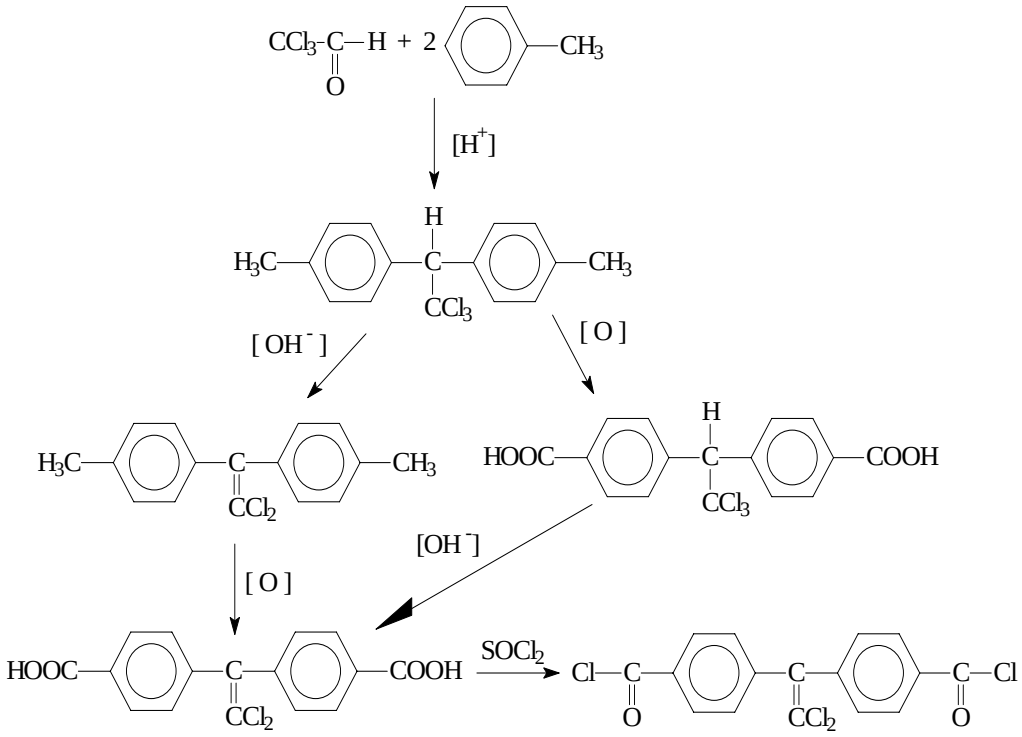

Scheme 2.

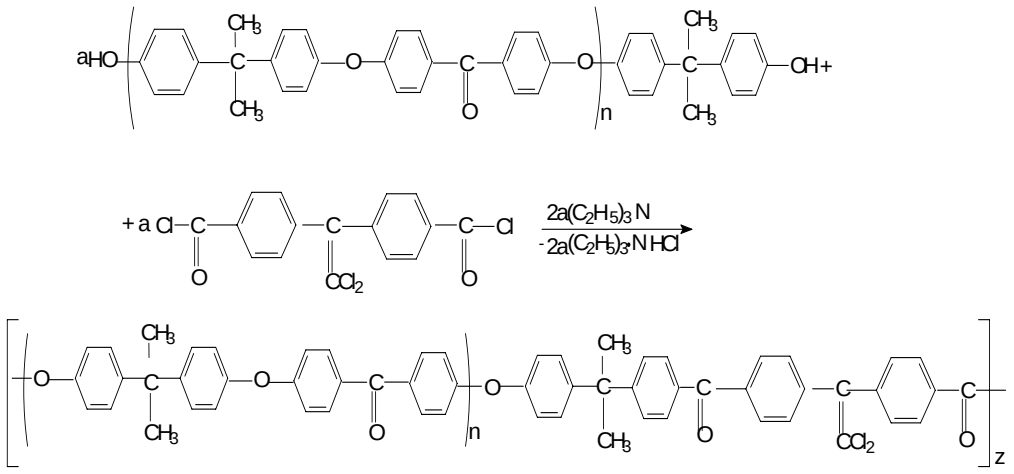

Scheme 3.

TEST METHODS

The experiments were conducted at a room temperature. The viscosity measurements were made according to GOST 10028-81 (Russian State Standards) using an Ubbelohde viscometer with a diameter of 0,34 mm. The viscosity was measured in 1,2-dichloroethane and the density of the solution was 0,5g/dl.

Poly(arylene ether ketone)s were investigated aiming at definition the possibilities of their use as construction materials. Mechanical properties of film PAEK specimens (100mm x l0mm x 0,lmm) were tested (GOST 17-316-71) on a MRS-500 with a constant strain rate of 40 mm/min at 20°C. The film specimens were obtained by pouring the polymeric solution into 1,2-dichloroethane.

The poly(arylene ether ketone)s structures were confirmed from the data of elemental analysis and infrared spectroscopy. Infrared spectra of olygomers and polymers were taken from peels and films with the use of IK-Fuye FTJR-850 spectrophotometer (Shimadzu, Japan);'windows from KBr, stratum 0,05 mm.

The molecular masses of poly(arylene ether ketone)s were measured by sedimentation in an ultracentrifuge "MOM" (type 317 B) through the balance approach technique.

Thermo-gravimetric analysis of poly(arylene ether ketone)s was performed on the derivatograph "MOM" under a temperature increase rate at 5 degree/min in the atmosphere (MOM is the abbreviation of the Hungarian company that manufactured the derivatograph).

The investigation of the polydispersity of the block copolymers was conducted by the turbidimetric titration method on an FEC-56M device. The principle of titration is that the diluted polymeric solution will become turbid if a precipitator is added and will have a different optical density from the original solution. The density of the solution was 0,01 g/ml. 1,2-dichloroethane was used as a solvent, and isopropyl alcohol - as precipitator.

Investigations of thermomechanical properties of the film specimens were carried out on a device thermo-mechanical analyzer. The temperature was increased at the rate of 4 degree/min and the load was kept to give a constant stress value of 0,05 MPa. The thickness and width of the test specimens were 0,1 mm and 8 mm, respectively, while the distance between the clamps was 80 mm. A thermal camera with a diameter of 30 mm and length of 150 mm was employed. The temperature gradient of the thermal camera was 2 degree along the length and 0,1 degree along the diameter. The deformation of the specimen was measured using a strain gauge.

The tests of the dielectric properties of poly(arylene ether ketone)s were carried out at a set with a Kumetre VM-560 Tesla machine at a frequency of 10^6 Hz. The values of dielectric permeability and tan δ of the dielectric loss angle were found for all specimens over the temperature range 20-300 °C.

Investigation of chemical resistance of poly(arylene ether ketone)s was carried out on the film specimens in the shape of a disk with a diameter of 5 sm. The specimens were tested in aggressive environment at 20°C for 16 days (384 hours). The specimens were measured every 12 hours.

The thermal -resistance was tested on the film specimens (strips) fixed vertically in a cylindrical camera, and laminar stream of nitrogen and oxygen mixture of the given correlation was put through it. The investigation was carried out under various

structures of the gas mixture unless the optimal structure, which provided burning of the specimen was found. Thermal-resistance was evaluated by the percentage of oxide, contained in the specimen (GOST 21207-75).

RESULTS AND DISCUSSION

The obtaining of poly(arylene ether ketone)s of the expected structure was confirmed by the data of infrared spectroscopy. The presence of the absorption bands which correspond to ether bonds, isopropylidene groups, diarylketone groups, $Ar_2C=C$, and the absence of the absorption bonds of corresponding hydroxyl groups points to the fact that polycondensation of olygoketones and dichloroanhydride 1,1-dichloro-2,2di-(4-carboxyphenyl) ethylene was thoroughly completed (figure 1).

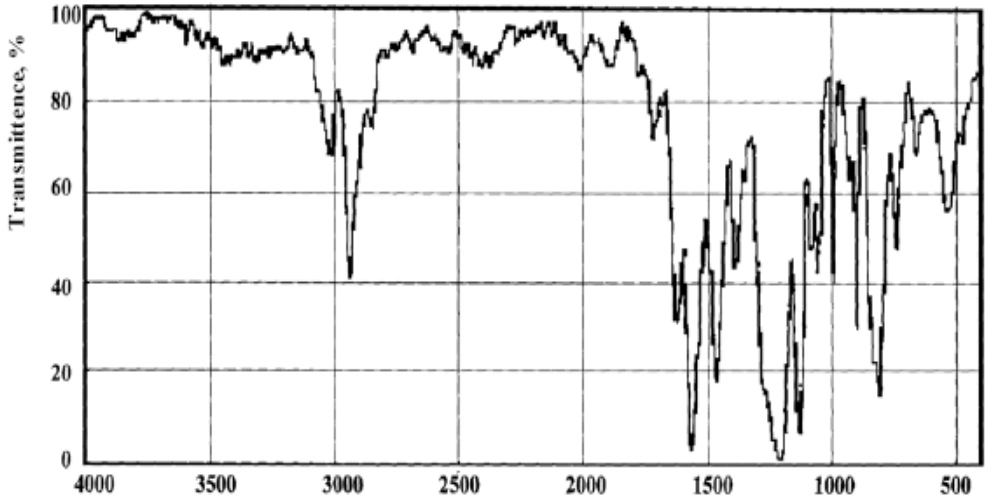

Figure 1. IR spectrum PAEK obtained from OK-20D.

The obtained PAEK is characterized by a high viscosity (*table 2*).

The results of turbidimetric titration also confirmed the structure of the above mentioned polymers. This fact was documented by the presence of only one maximum on the differential curves which means that the polymer reactants were statistically mixed (figure 2).

Table 2. Some properties of PAEK

PAEK obtained from	Intrinsic viscosity (m^3/kg)	Molecular weight x 10^3	T_g (^0C)	σ_{break} MPa	ε, %	Oxygen Index, %	Mass loss temp. (^0C)			
							$T_{2\%}$	$T_{10\%}$	$T_{50\%}$	$T_{2*\%}$
OK-1D	0,078	80	200	72,5	14,5	35,5	367	430	560	392
OK-5D	0,075	70	190	74,5	13,6	32,0	372	438	557	390
OK-10D	0,049	47	182	78,7	11,2	31,0	376	464	567	390
OK-20D	0,040	40	175	82,7	8,10	30,5	388	512	583	400

T_2*%- the PAEK loss in mass after thermal treatment at 300 °C for 30 minutes.

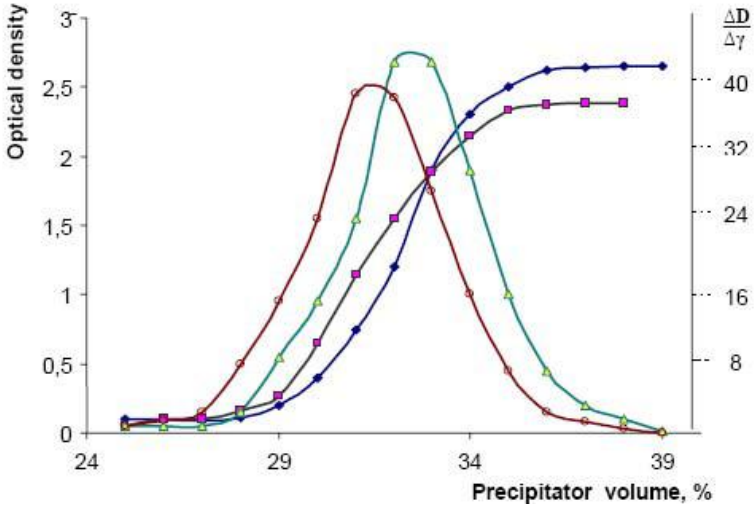

Figure 2. The turbidimetric titration curves of PAEK obtained from OK-1D (♦, Δ) and PAEK obtained from OK-20D (■,○); integral curves (♦,■), differential curves (Δ,○).

All the poly(arylene ether ketone)s, obtained were well dissolved by 1,2-dichloroethane, chloroform, tetrahydrofuran, etc.

The molecular weights of poly(arylene ether ketone)s were found to be in the interval 40000-80000. The highest molecular weight values correspond to poly(arylene ether ketone)s on the basis of short olygoketones, which confirms their high activity.

The thermomechanical tests showed that the values of the glass transition and of fluidity temperature of these polymers depended on the presence of a great number of simple flexible ethereal bonds in their macro chains. The portion of simple ethereal bonds in the chain becomes higher with the increase of length (condensation degree) of olygoketones, which provides decreased T_g and T_f of these polymers. PAEK on the basis of OK-20D, where the portion of ether bonds is the highest, and the portion of dichloroanhydride 1,1-dichloro-2,2di-(4-carboxyphenyl)ethylene remnants in the chain is the lowest, possesses the structure, closest of to that of olygoketones, and the latter has a low glass transition temperature. In the case of PAEK, based on OK-ID, higher T_g defined by the most "severe" component - dichloroanhydride 1,1-dichloro-2,2di-(4-carboxyphenyl)ethylene.

The comparative analysis of the poly(arylene ether ketone)s thermal properties shows that with the increase of the initial olygomers length, a significant increase of thermal-resistance is observed. This kind of changes of thermal-resistance can be explained by the fact that, on the one hand, a saturation of polymeric chain by thermal-resistant stable ether bonds is observed, and on the other hand, the portion of non-stable ester bonds, that are brought in by the remnants of dichloroanhydride 1,1-dichloro-2,2di-(4-carboxyphenyl)ethylene, decreases abruptly. Moreover, with the increase of polycondensation degree of the initial olygoketones the packing density of polyetherketones increases. It is obvious, that these three factors promote to the growth of thermal-resistance of these poly(arylene ether ketone)s.

The data obtained from thermo-gravimetric analysis have shown that in case of thermal oxidizing destruction of PAEK, processes of intensive structuring are observed simultaneously with decomposition reactions, and this peculiarity is connected

with the presence of group >C=CCl_2 in the structure of the given polymers, which is able to connect with the disclose of double bonds, what causes the destruction process lowering .

Under the investigation of a number of other properties, including infrared spectroscopy of specimens, passed thermal treatment, the structuring of aromatic unsaturated poly(arylene ether ketone)s according to the place of a double bond is confirmed by the *scheme 4*:

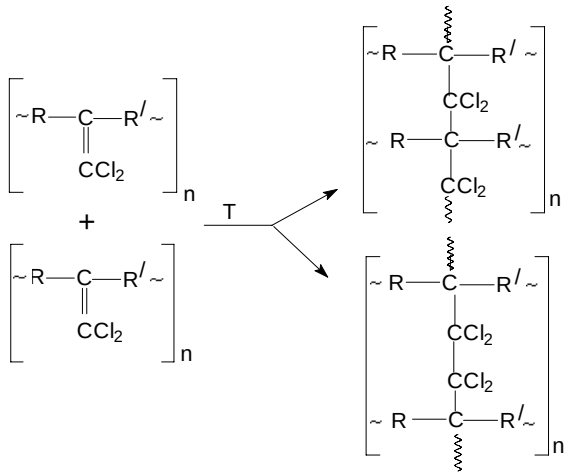

Scheme 4.

The investigation of thermal-resistance of PAEK specimens, kept preliminarily for 30 minutes at 300°C, has shown a significant increase of temperatures of loss of 2% of mass (table 2), which is strongly marked for poly(arylene ether ketone)s based on OK-lD and OK-5D.

For poly(arylene ether ketone)s with a less quantity of double bonds in macro chains thermal treatment has less effect. This phenomenon confirms, that some properties of poly(arylene ether ketone)s may be increased by an optimal choice of thermal treatment.

By their strength properties the given unsaturated poly(arylene ether ketone)s can be compared with the similar PAEKs on the basis of dichloroanhydrides of isophthalic and terephthalic acids. However, it must be noticed that the presence of a double bond in the structure of the given poly(arylene ether ketone)s gives an opportunity to increase the resources of these polymers. Thus, thermal treatment of PAEK on the basis of OK-ID under the pointed above conditions allowed to increase the value of the breaking strength up to 90 MPa, preserving the relative lengthening at the 10% level.

As it was expected, the given PAEK, as well as halogen -containing polyethers, possesses a high thermal-resistance. The obtained data show that poly(arylene ether ketone)s, which are more saturated by the chlorine atoms, are characterized by a higher level of their oxygen indices. All the obtained poly(arylene ether ketone)s are related to the self-damping polyethers.

The investigation of dielectric permeability (ε') and tan of the dielectric loss (tan δ) has shown that these indices are not high and relatively stable in a glassy condition. The insignificant fall of ε' from 3,5 to 3,3 under transition from PAEK on the basis of OK-ID to the ones on the basis of OK-20D, may be connected both with the lowering of the

macro chain capacity for dipolar orientation, and the decrease of contents of the polar group C = CCI_2 in the macro chain.

The further increase of temperature facilitates the dipolar polarization by the decrease of the environment viscosity. The curve and dipoles orientation is accompanied by a loss of energy and tan δ increases. However, when a certain temperature is reached, the viscosity of the environment decreases and the loss of energy reduces too. The curves (*see figure 3*) show that with the increase of length of initial olygoketones, maximums on the curves, which are related to α-process, displace to the side of lower temperatures, and it is corresponded with the thermo-mechanical analysis data.

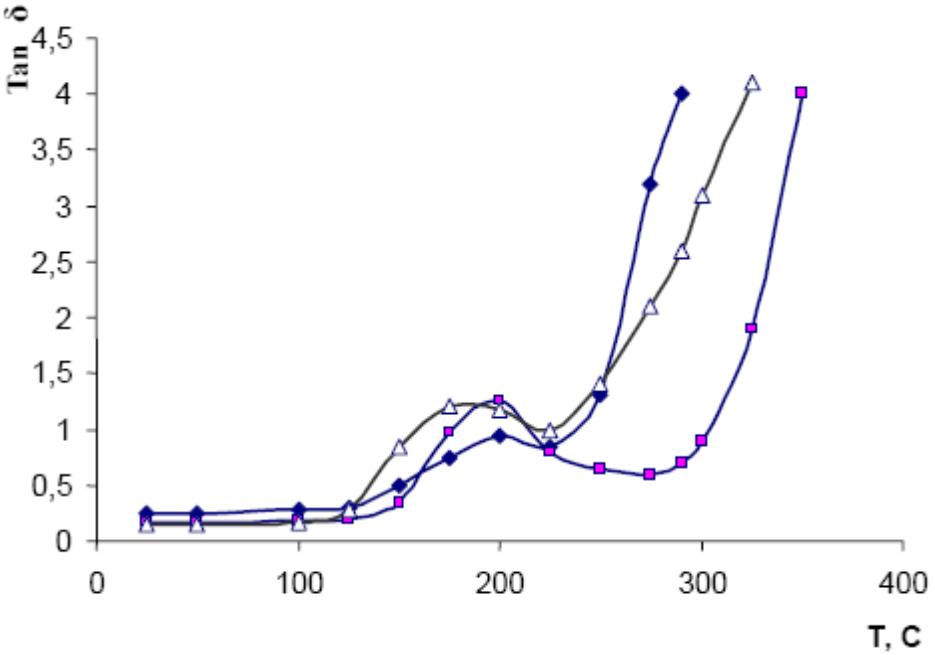

Figure 3. The relationship between the tan δ and temperature for PAEK obtained from OK-1D (♦), OK-10D (■) and OK-20D (Δ).

Due to the fact that constructional polymeric materials are often used in aggressive environment, the obtained poly(arylene ether ketone)s were tested for resistance to different acids and alkali. The tests showed (see table 3), that PAEK demonstrate a good resistance to the diluted mineral acids and to the concentrated hydrochloric acids. However, the poly(arylene ether ketone)s are easily dissolved both in the diluted and in the concentrated alkali, which may be connected with the presence of the chemically, non-stable complex-ethereal bonds in macro chains of the poly(arylene ether ketone)s.

Table 3. Chemical stability of PAEK

PAEK obtained from	Exposure time (h)	Weight variations (%)				
		Diluted acid (H_2SO_4)		Diluted alkali (NaOH)		Conc. acid (HCl)
		10%	30%	10%	30%	
OK-1D	24	0,38	0,34	0,93	0,39	0,74
	48	1,04	0,98	2,59	-0,55	1,64
	96	1,71	1,82	2,71	-1,84	2,85
	384	1,87	1,29	-0,12	-9,68	2,91
OK-10D	24	0,33	0,29	0,90	0,32	0,65
	48	0,51	0,54	1,82	-0,62	1,62
	96	1,22	1,27	2,24	-1,74	2,18
	384	1,25	1,26	1,03	-7,19	2,29
OK-20D	24	0,14	0,19	0,87	0,22	0,14
	48	0,39	0,44	1,69	-0,52	1,52
	96	0,74	0,99	1,97	-0,91	1,91
	384	0,85	1,14	1,65	-5,92	2,07

CONCLUSION

Poly(arylene ether ketone)s on the basis of olygoketones with different condensation degrees and dichloroanhydrides l,l-dichloro-2,2-di(4-carboxylphenyl) ethylene were obtained. It was shown that poly(arylene ether ketone)s were characterized by high indices of stability. They are not flammable, they show high resistance to the diluted mineral acids. It was also shown, that a number of common features of poly(arylene ether ketone)s may be improved by thermal treatment due to the presence of unsaturated bond in the macro chain. The dependence of change of poly(arylene ether ketone)s properties on their condensation degree of the initial olygoketones was confirmed.

The used research methods are precise and reliable.

REFERENCES

[1] Shaov A.H., Charayev A.M., Mikitaev A.K., Kardanov A.Z. Khasbulatova Z.S. Aromatic polyethers and polyetherethers, *Plastich. Massy.*, 11, 14 (1990).

[2] Charayev A.M., Shaov A.H., Mikitaev A.K., Matvelashvili G.S., Khasbulatova Z.S. Polymeric composite materials on a basis polyetherethers, *Plastich. Massy*. 3, 3 (1992).

[3] Charayev A.M., Shaov A.Kh., Shustov G.B., Mashukov N.I. Blok copolyetherketons, Third Russian-Chinese Simpo-sium *" Advanced materials and processes "*, Kaluga, Russia, 245, (1995).

[4] Sharapov V.V., Shaposhnikova V.V., Salaskin S.N. Influence of conditions of polycondensation on synthesis polyarylenetherketones, *Vysokomolek. Soed.,* 45, 113, (2003).

[5] Ozden S., Charayev A.M., Shaov A.H. The synthesis of polyetheretherketones and investigations of their properties. *J. Mater. Sci*.- 34, 2741, (1999).

[6] Ozden S., Shaov A.H., Charayev A.M., Bidanikov A.Y. Compositions Based in Aromatic Block Copolyester and p-Bytoxyphenyl Cyclohexyl Phosphinic Acid.- *Polym. and polym. Comp*.-1998.-Vol. 6.- № 2.- P.103-107.

[7] Ozden S., Charayev A.M., Shaov A.H., Shustov G.B. Synthesis and Assessment of the Properties of Polyetherketones (PEK) Based on Olygoketone-phenolphtaleines (OKPP)-Polyester Blok Copolymers.- *J. Appl. Polym. Sci*.. 68. 1013 (1998).

[8] Charayev A.M., Shaov A.H., Shustov G.B. Mikitaev A.K. Synthesis and Properties of Polyetheretherketones –*Chemistry and chemical technology*.- 41, 78 (1998).

[9] Osden S., Shaov A.H., Charaev A.M., Gurdaliyev X.X.. The effects of p-butoxy-phenylcyclohexylphosphinic acid on the properties of PC based on bisphenol A.- *J. Appl. Polym. Sci.* 80, 2113 (2001).

[10] Ozden S., Shaov A.H., Charayev A.M., Mikitaev A.K., Bedanokov A.Y. Aromatic block copolyesters stabilised with metallic salts of phosphinic acid.- *Polymers and Polymer Composites.* 9, 213 (2001).

[11] Ozden S., Charaev A.M., Shaov A.H. High impact thermally stable block copolyethers.- *J. Mater. Sci.* 36, 4479 (2001).

[12] A.Kh. Shaov, N.N. Amerkhanova, A.M. Kharayev. Phosphorous Organic Compounds as the stabilizers of the Aromatic Blockpolyethers.–Aging of polymers, polymer blends and polymer composites. – *Nova Sci. Publ.* – New York. – 2002.- Vol. 2.- pp. 161-166.

[13] S. Ozden , A. M. Charayev, A. H. Shaov. Synthesis of block copolyetherether ketones and investigations of their properties.- *J. Appl. Polym.* Sci. 85, 485 (2002).

[14] Patent №1736128 (USSR)

[15] Yanota H., Alov E.M., Moskviechev YU.F., Mironov G.S. *J. Org. Himii*, 21, 365 (1985).

In: Monomers, Oligomers, Polymers, Composites… ISBN: 978-1-60456-877-6
Editors: R. A. Pethrick, G.E. Zaikov et al.

Chapter 8

THE ETHANOL INFLUENCE ON ACRYLIC ACID POLYMERIZATION KINETICS AND MECHANISM IN INVERSE EMULSIONS STABILIZED BY LECITHIN

S.A. Apoyan, R.S. Harutynnyan, J.D. Grigoryan and N.M. Beylerian
Yerevan State University; E-mail: norbey@ysu.am

ABSTRACT

The functions which describe the dependence of polymerization rate (R_{pol}) of acrylic acid (AAc) initiated with potassium persulfate (PP) in inverse emulsions stabilized by lecithin (Le) in presence of ethanol (Et) on $[Et]_0$ and $[Le]_0$ are bell shape curves.

$R_{pol} \sim [PP]_o^n [AAc]^m$. With increase of $[Et]_0$ n increases from 0.5 to 1. m=1 when $0 < [AAc] \leq 1M$. With increase of $[AAc]_o$ more than 1M m decreases striving 0. Both phenomenons are explained. It is established that the polymerization initiation rate (R_{in}) does not depend on both $[Et]_o$ and $[Le]_o$. They have considerable influence on colloid-chemical properties of the emulsion assisting to R_{pol} increase.It is concluded that the coexistence of Et +Le displays simultanously positive and negative effects which condition the appearance of maximums on curves $R_{pol} = f([Et]_o)$ and $R_{pol} = f([Le]_o)$ functions.

INTRODUCTION

The influence of some aliphatic alcohols on kinetics of styrene and chloroprene polymerization kinetics is studied [1-3]. In particular it has been established that alcohols are chain transfer agents, so they are being used to regulate the mean molecular masses (MMM) of obtained polymers. Apart it is shown that they influence on colloid-chemical properties of polymerization systems. So by this means they act on the over-all polymerization kinetics.

In [4] it is shown that in the case of AAe polymerization initiated with PP in inverse emulsions (IE) stabilized by Le in a more extent unsoluble polyAAe is being obtained.

Taking into consideration data presented [1-4] it is assumed to use alcohols to obtain watersoluble polyAAe in IEs.

The aim of the present research-work is to study ethanol's influence on AAc's R_{pol} initiated with PP in IEs stabilized by Le, as well on obtained polyAAe MMM.

It is worthy to note that Et is not toxic and is available.

EXPERIMENTAL

R_{pol} is determined making use dilatometry. The volume ratio water/oil (toluene)=1:2=const. Water was bidistilled.

PP is recrystallized fivefolds from water solution. The purity was 99,8% (iodometric determination). Le was 10% ethanol solution ("standard" grade). The prepared Le initial solution was kept in oxygen-free medium in refrigerator. MMM is determined using viscositnetric method [5]. The following formulae is used: $[\eta]=6{,}6\cdot10^{-4}\cdot M^{0,5}$ at 243k and for 0,2% HCl solution of AAe.

The surface and interface tensions are determined by Rebinder's method[6] (determination of the maximal pressure in bubles).

The emulsion's stability has been determined at room temperature measuring the moving on of the separation boundary between two phases[7].

RESULTS AND DISSCUSSION

The curves depicted on fig.1 present the AAc R_{pol} and polyAAc MMM`S dependences on $[Et]_0$ in Absence of Le (1) and in its presence (2).

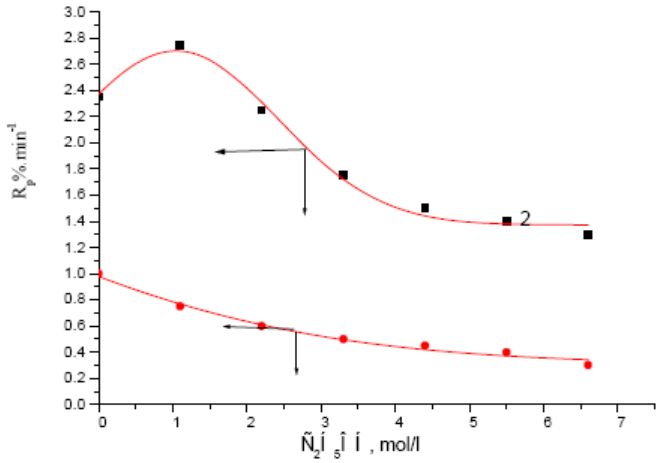

Figure 1. Dependence of AAc polymerization rate (R_{pol} in $\%\cdot min^{-1}$) and polyAAc MMM on $[El]_o$ (M) in absence (1) and in presence (2,3) of L. $[L]_o$=1% (2) and 0.5% (2,3). $[AAc]_o$ =1M, $[PP]_o = 2\cdot 10^{-3}$.

The curves depicted on fig.1 present the AAc R_{pol} and polyAAc MMM's dependences on $[Et]_o$ in absence and in presence of Le. In Le absence with increase in $[Et]_o$ R_{pol} decreases. But in presence of Le (1% in toluene) R_{pol} has maximum value at $[Et]_o$ =1M.

Same regularities are established for MMM=f($[Et]_o$). At $[Le]_o \leq 0,5\%$ and in presence of Et the obtained polyAAc is water soluble. MMM decreases with $[Et]_o$ increase. But increasing $[Le]_o$ the obtained polyAAe solubility decreases.

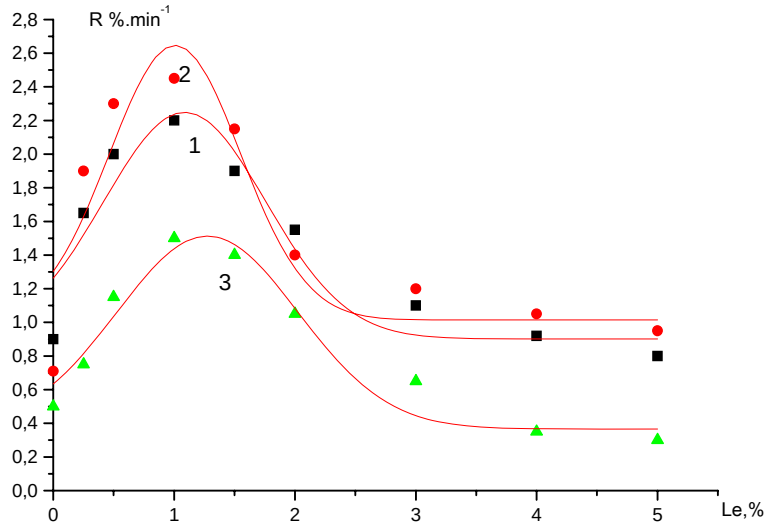

Figure 2. Dependence of R_{pol} on $[Le]_o$ in presence of different amounts of Et. $[Et]_o$: 0(1); 1,1 M (2) and 6,6(3) at $[AAc]_o$ = 1M, $[PP]_o = 2 \cdot 10^{-3}$.

The observed maximum corresponds to $[Le]_o$=1%. It depends on a few extent on $[Et]_o$. Further kinetic studies are carried out for this condition.

The study of R_{pol} dependence on $[PP]_o$ show that $R_{pol} \sim [PP]_o^{\ n}$, where n=f($[Et]_o$) (see table 1).

Table 1. R_{pol}'s dependence on $[PP]_o$ at $[Le]_o$=1% and 318K $[AAc]_o$=1M.

$[Et]_o$ / $10^3[PP]_oM$	0	1.1	6.6	
0.5	1.0	1.03	0.42	R_{pol} %·min^{-1}
1	1.35	1.58	0.8	
1.5	1.65	2.43	1.32	
2.0	2.20	2.65	1.52	
n	0.5	0.73	1.0	

These data show that in presence of Le with increase in $[Et]_o$ the mechanism of chain termination is being changed. In absence of Et the chain termination occurs by quadratic mechanism, while at $[Et]_o$ =6,6M it becomes linear.

The following step is the study of R_{pol} dependence on $[AAe]_o$ in presence of different amounts of Et.

The obtained data are summarized in table2.

Table 2. $[Le]_o$=1%, $[PP]_o=2\cdot10^{-3}$M, V_w/V_{tol} =1:1, T=318K

$[Et]_o$ / [AAc]M	0	1.1	6.6	
0.5	1.3	1.5	0.5	R_{pol} %·min^{-1}
0.75	1.8	2.0	1.0	
1.0	2.2	2.65	1.52	
1.5	2.3	2.82	1.9	
2.0	2.5	2.95	1.95	

From data presented in table 2 it follows that $R_{pol}\sim [AAc]^m$. It is easy to show that when $[AAc]_o\leq 1$M m=1. But when $[AAc]_o>1$M m tends to 0.

To explain this regularity at first the R_{in} dependence on $[Et]_o$ end $[Le]_o$ has been studied. Inhibitory method has been used to determine R_{in}. The inhibitor was TEMPO.

Obtained kinetic data unambiguously show that R_{in} does not depend on $[AAc]_o$, [Et] and $[Le]_o$. These results are in full accordance with data obtained earlier [8-10]. So the primary radicals are being formed in the water phase as result of persulfate dianion monomolecular decomposition.

Therefore , Et and Le may influence on chain propagation , termination and transfer reactions. But the following circumstance must be considered too.

As was mentioned the polymerization is being carried out in IE. Principally the influence of Et and Le on the emulsion colloid-chemical properties may not be excluded. Data given in table 3 confirm the expressed assumption.

Table 3.

$[C_2H_5OH]$ M	T_{ss} min	σ dyne/cm		[AAc] %	
		$[Le]_o$=0%	$[Le]_o$=1%	In water	In toluene
0	6	34.4	11.5	70	30
1.1	8	22.9	9.5	66	34
6.6	14	5.7	5.0	50	50

$[AAc]_o$=1M , VH_2O: V $C_6H_5CH_3$ =1:1, T=303K.

t_{ss} – is the emulsion semidecay time, σ – the surface tension. It is obvious that Et increases the emulsion stability. On the other hand they both diminish the surface tension which results in decrease of micelles size , which in its turn must result in enhance of micelles(the polymerization loci) number on which depends R_{pol} . This is the positive influence of the Et + Le mixture on R_{pol}.

But at the same time that mixture displays also a negative influence on R_{pol} , as well on MMM. It is due to the fact that they both efficiently transfer the chain , in the case of Le- with degradation. This may be the reason why at high concentration of Et , when Le solubility in the water phase may be increased , the chains are being terminated by linear mechanism.

What which conceurns the peculiar dependency of R_{pol} on$[AAc]_o$, one cane say the following.

The main polymerization loci is the water phase. It is well know that all carbonic acids , AAc too, form dimers :2AAc↔dimer. It is obvious that the dimer is less polar than the monomeric acid. So it is more probable that the dimer molecules cross from the water phase into the "oil".

If $[AAc]_o$ is the AAc's initial concentration , so a part of AAc molecules will be dimerized resulting in decrease of AAe's real concentration ([AAc]real)(see table 3). As was mentioned both forms of AAc are in equilibrium. So ; $[AAc]_{real}$ =$[AAc]_o$- [dimer]. In the propagation reaction takes part monomerie molecules of AAc , which concentration in the reaction zone (in the water phase) is equal to $[AAc]_{real}<[AAc]_o$. It is easy to note that increasing $[AAe]_o$ $[AAc]_{real}$ may be increased only in a very few extent. Probably for this reason increasing $[AAc]_o$ the reaction order with respect to acrylic acid tends to zero.

REFERENCES

[1] Storoge Gu. F., Yurjenko A.U., Coll.J., 1963.v.25, No,p.77(in Russion)

[2] Harutunian R.S., Beylerian N.M., Trans. of Yerevan State University, 1982, N2, p. 79(in Russian)

[3] Harutyunyan R.S., Dissertation (for PhD degree), Yerevan, 1984 (in Russia)

[4] Apoyan S.H., Grigorian J.D., Harutyunyan R.S., Beylerian N.M., Physical chemistry of Polymers, Coll. of scientific papers, 'Tver state university (in Russian), 2004, issue10, c.79

[5] Rafikov S. R., Pavlova S.A., Tverdekhlebova I.I., Methods to determine molecular weights and polydispersity of highmolecular compounds, Moscow, Ed.ofURSS Academy of Sciences, 1963, p.301.

[6] Ayvazian V.B., Textbook for practical works in chemistry of surface phenomenon and adsorption, Moscow, Ed. of High School, 1973, p.19.

[7] Poustovalov N.N., Poushkarev V.V., Berezok V.G, Coll.J.,1974 v.36,N 1, p. 171

[8] Chaltikian H.H., Khachatrian A.Gu., Beylerian N.M., Kinetika I kataliz , 1971, v,12,N4, p. 1049(in Russia)

[9] Beylerian N.M., Khachatrian A.Gu., Chaltikyan H.H., *Armenian chem.. J.*, 1970,v,23,N7, p.575(in Russia)

[10] Beylerian N.M., *Acta Polymerica*, 1982,v,33,N5, p.339.

In: Monomers, Oligomers, Polymers, Composites… ISBN: 978-1-60456-877-6
Editors: R. A. Pethrick, G.E. Zaikov et al.

Chapter 9

SMOOTHED PARTICLE HYDRODYNAMICS (SPH) ALGORITHM FOR NUMERICAL FLUID-STRUCTURE INTERACTION STUDIES IN POROUS MEDIA – NEW TRENDS AND ACHIEVEMENTS

N. Amanifard and A. K. Haghi*
University of Guilan, P. O. Box 3756, Rasht, Iran

ABSTRACT

In this chapter, SPH (Smoothed Particle Hydrodynamics)has been introduced to investigate pore-scale flow phenomena in porous media . Using this approach, fluid velocity and pressure distributions, discharge velocity, and fluid particle paths can be computed, as well as other information that would be difficult or impossible to observe experimentally

1. INTRODUCTION

Numerical methods applied to porous media flow include finite difference methods [1], finite element methods [2-6], and boundary integral methods [7,8]. It can be difficult, however, to apply such methods to flows involving immiscible fluids or mobile solid boundaries. Lagrangian particle techniques, such as smoothed particle hydrodynamics (SPH) and lattice Boltzmann [9], provide an alternative approach which is more easily applied to such problems.

SPH has been used to investigate pore-scale flow phenomena in porous media [10-13]. The SPH method firstly, developed for astrophysical applications [14, 15], and it is a fully Lagrangian and mesh-less. Using this approach, fluid velocity and pressure distributions, discharge velocity, and fluid particle paths can be computed, as well as other information that

* Corresponding author e-mail: Haghi@Guilan.ac.ir

would be difficult or impossible to observe experimentally. SPH has certain advantages over other fluid dynamical methods, which may encounter difficulty with deformable boundaries, multiphase flows, free surfaces, and the extension to three dimensions. For example, if the soil grains which form a porous structure are allowed to move in response to fluid flow, other techniques may require continual remeshing of the flow domain, leading to increased numerical diffusion and algorithmic complexity. In addition, SPH uses an interpolation method which simplifies the inclusion of chemical and thermal effects.

While SPH is versatile, errors can sometimes be larger than those obtained using grid-based methods tailored for specific problems. Moreover, SPH can be computationally expensive for certain applications. For example, individual time-steps for comparable numbers of nodes with SPH and finite element methods take similar computational effort. However, many more steps are typically required by SPH to obtain a solution to steady-state problems. For time-dependent problems at low Reynolds number, the computational effort is similar to a finite element method employing explicit time integration.

The computational expense of SPH is in part a consequence of its versatility.

More specialized numerical techniques employ computational nodes which have relatively small regions over which they interact. For Eulerian methods, these regions remain fixed throughout the computation (provided nodes are not added or deleted). In addition, the weights associated with nodes are often time-independent.

The adaptive smoothed particle hydrodynamics (ASPH) is introduced by Owen et al., (1998) and Fulbright and Benz,(1995), and has been developed for microchannel studies as a novel attempt by Liu and Liu (2005).

As a mesh-free particle Lagrangian method, SPH has special advantages, and has been extended to different areas with various applications (Liu et al., 2002; 2003a;b). It can naturally determine the location of non-homogeneities, free surfaces, and moving interfaces. With SPH, the nodes (particles) are free to move, producing variations in the nearest neighbors of each particle. Thus, the weights associated with particle interactions are time-dependent and must be recalculated at each time step. The word "particle" does not mean a physical mass instead it refers to a region in space. Field variable are associated to these particles and at any other point in space are found by averaging, or smoothing, the particle values over the region of interest. This is fulfilled by an interpolation or weight function which is often called the interpolation kernel. It should be pointed out that SPH method was then successfully applied to the study of various fluid dynamics problems, such as free-surface incompressible flows [19], and viscous flows [20,21]. Since the early 1990s, SPH was applied also to the simulation of elasticity and fragmentation in solids. SPH has been also used to simulate the interaction between different fluids [18, 22], different solids [23] and between fluids and structures [24] in presence of explosions.

The objective of this chapter is to perform a fundamental base on numerical observations by the SPH algorithm in microchannels and porous media problems, and the authors believe that it can be used with some further studies for a wide range of Knudson numbers from continuous approach to the particle-molecular flow zones.

2. BASIC CONCEPTS

The SPH method is based on the interpolation theory. The method allows any function to be expressed in terms of its values at a set of disordered points representing particle points using a kernel function. The kernel function refers to a weighting function and specifies the contribution of a typical field variable, $\mathrm{A(r)}$ at a certain position, r in space. The kernel estimate of $\mathrm{A(r)}$ is defined as [28]:

$$\left\langle \mathrm{A}_h(r)\right\rangle = \int_{Space} \mathrm{A}(r')\ W(r-r',h)\ dr' \tag{1}$$

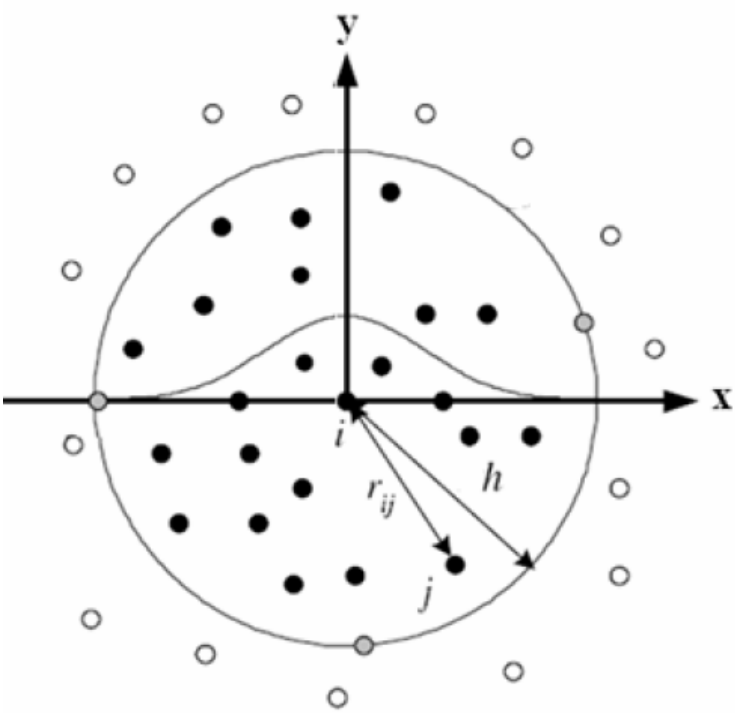

Figure 1. SPH Characteristics in a two-dimensionl space. Th smoothing length *h* which the gives the boundaries of domain of influence is shown.

Where the smoothing length h represents the effective width of the kernel and W is a weighting function with the following properties[28]:

$$\int_V W(r-r',h)\ dr' = 1 \quad \lim_{h\to 0} W(r-r',h) = \delta(r-r') \tag{2}$$

If $A(r')$ is known only at a discrete set of N point $r_1, r_2, ..., r_N$ then $A(r')$ can be approximated as follows [28]:

$$A(r') = \sum_{j=1}^{N} \delta(r' - r_j) A(r_j) (dV)_j \tag{3}$$

Where $(dV)_j$ is the differential volume element around the point r_j. Combining Eq. (1) and Eq(3) yields[28]:

$$\langle A_h(r) \rangle = \sum_{j=1}^{N} \int \delta(r' - r_j) A(r_j) (dV)_j W(r - r', h) dr' \tag{4}$$

After integration, and replacing the differential volume element $(dV)_j$ by m_j / ρ_j one gets [28]:

$$\langle A_h(r) \rangle = \sum_{j=1}^{N} \frac{m_j}{\rho_j} A_j W(r - r', h) \tag{5}$$

Where the summation index j denotes a particle label and particle j carries a mass m_j at position r_j, a density ρ_j and a velocity v_j. The value of A at $j-\mathrm{th}$ particle is shown by A_j. The summation is over particles which lie within a circle of radius $2h$ centered at r.

2.1. Kernel Function

The kernel function is the most important ingredient of the SPH method. Various forms of kernels with different compact support were proposed by many researches. Recently studies [21-23] indicate that stability of SPH algorithm depends strongly upon the second derivative of the kernel.

Using different kernel in SPH method is similar to using different schemes in finite difference methods. One of the most popular kernels is based on spline functions [23]:

$$W(r,h) = \frac{\sigma}{h^{\nu}} \times \begin{cases} 1 - \frac{3}{2}s^2 + \frac{3}{4}s^3 & 0 \le s < 1 \\ \frac{1}{4}(2-s)^3 & 1 \le s < 2 \\ 0 & 2 \le s \end{cases} \qquad s = \frac{|\mathbf{r}|}{h} \tag{6}$$

Where ν is number of dimensions and σ is normalization constant with the values: $\frac{2}{3}, \frac{10}{7\pi}, \frac{1}{\pi}$ in one, two and three dimensions respectively. This kernel has compact support which is equal to $2h$, it means that interactions are exactly zero for $r > 2h$.The second derivatives of this kernel is continues and the dominant error term in the integral interpolant

is $O(h^2)$. Higher order splines can be used, but they interact at further distances and thus require more computational time.

2.2. Gradient and Divergence

The gradient and divergence operators need to be formulated in a SPH algorithm if simulation of the Navier-Stokes equations is to be attempted. In this work, the following commonly used forms are employed for gradient of a scalar A and divergence of a vector u [29]:

$$\frac{1}{\rho_i}\nabla_i A = \sum_j m_j \left(\frac{A_i}{\rho_i^{\,2}} + \frac{A_j}{\rho_j^{\,2}} \right) \nabla_i W_{ij} \tag{7}$$

$$\frac{1}{\rho_i}\nabla_i . \mathbf{u}_i = \sum_j m_j \left(\frac{\mathbf{u}_i}{\rho_i^{\,2}} + \frac{\mathbf{u}_j}{\rho_j^{\,2}} \right) \nabla_i W_{ij} \tag{8}$$

Where $\nabla_i W_{ij}$ is gradient of kernel function $W(|r_i - r_j|, h)$ with respect to r_i, the position of particle i. This choice of discretization operators ensure that an exact projection algorithm is produced.

2.3. Laplacian Formulation

A simple way to formulate the Laplacian operator is to envisage it as dot product of the divergence and gradient operators. This approach proved to be problematic as the resulting second derivative of the kernel is very sensitive to particle disorder and can easily lead to pressure instability and decoupling in the computation due to the co-location of the velocity and pressure. In this paper, the following alternative approach is adopted [30]:

$$\nabla . \left(\frac{1}{\rho} \nabla A \right)_i = \sum_j m_j \frac{8}{(\rho_i + \rho_j)^2} \frac{A_{ij}\, r_{ij} . \nabla_i W_{ij}}{|r_{ij}|^2 + \eta^2} \tag{9}$$

Where $A_{ij} = A_i - A_j$, $r_{ij} = r_i - r_j$ and η is a small number introduced to avoid a zero denominator during computations and is set to $0.1h$.

3. GOVERNING EQUATIONS

In this chapter a new algorithm for elastic deformation modeling of solid particles is presented which doesn't utilize any artificial viscosity and artificial stress terms. The proposed algorithm for solid particles modeling is completely compatible with fluid particles and it Permits to easily follow the motion of fluid–solid interface in time without any specific treatment.

3.1. Governing Differential Equations for Fluid Particles

The governing equations for transient compressible fluid flow include the conservation of mass and momentum equations. In a Lagrangian framework these can be written as:

$$\frac{1}{\rho}\frac{D\rho}{Dt}+\nabla.\mathbf{V}=0 \tag{10}$$

$$\frac{D\mathbf{V}}{Dt}= g + \frac{1}{\rho}\nabla.\overset{\Rightarrow}{\tau} - \frac{1}{\rho}\nabla P \tag{11}$$

Where t is time, g is the gravitational acceleration, P is pressure, V is the velocity vector , $\overset{\Rightarrow}{\tau}$ is viscous stress tensor and D/Dt refers to the material derivative. The density ρ has been intentionally kept in the equations to be able to enforce the incompressibility of the fluid. The momentum equations include three driving force terms, i.e., body force, forces due to divergence of stress tensor and the pressure gradient. These must be handled along with the incompressibility constraint. In a SPH formulation the above system of governing equations must be solved for each particle at each time-step. The sequence with which the force terms are incorporated can be different from one algorithm to another.

3.2. Viscous Terms in Fluid Zone

It is known that In the Newtonian fluids, $\overset{\Rightarrow}{\tau}$ in equation (11) must be defined as below:

$$\overset{\Rightarrow}{\tau}=2\mu\,\mathbf{D} \tag{12}$$

$$\mathbf{D}=\tfrac{1}{2}\left(\nabla\mathbf{v}+\nabla\mathbf{v}^{t}\right) \tag{13}$$

$$\mathbf{v} = u\,\vec{i} + v\,\vec{j} \tag{14}$$

$\vec{\tau}$ in the momentum equation appears as a divergence form which can be written in SPH formulation as below (the details of this formulation was presented in my last paper)

$$\left(\frac{1}{\rho}\nabla.\vec{\tau}\right)_i = \sum_j m_j\left(\frac{\vec{\tau}_i}{\rho_i^{\,2}} + \frac{\vec{\tau}_j}{\rho_j^{\,2}}\right).\nabla W\left(\vec{\mathbf{r}}_i - \vec{\mathbf{r}}_j, h\right) \tag{15}$$

3.3. Governing Differential Equations for Elastic Solid Zone

The acceleration equations (Momentum equation) for Elastic Medium can be written as below [26]:

$$\frac{\mathrm{d}\mathbf{V}}{\mathrm{d}t} = g + \frac{1}{\rho}\nabla.\vec{\sigma} \tag{16}$$

In above equations d/dt denotes a derivative following the motion, σ is the stress tensor and can be written as [26]:

$$\sigma^{ij} = -P\delta^{ij} + S^{ij} \tag{17}$$

By Combining Eq. (16) and Eq. (17) the final form of governing equations for Elastic Medium Motion includes the continuity and the acceleration equations can be written as below

$$\frac{1}{\rho}\frac{D\rho}{Dt} + \nabla.\mathbf{V} = 0 \tag{18}$$

$$\frac{\mathrm{d}\mathbf{V}}{\mathrm{d}t} = g + \frac{1}{\rho}\nabla.\vec{S} - \frac{1}{\rho}\nabla P \tag{19}$$

Where g is the gravitational acceleration, P is pressure, $\vec{S}$ is the deviatoric stress tensor and its rate of change is given by:

$$\frac{\mathrm{d}S^{ij}}{\mathrm{d}t} = 2\mu\left(\dot{\varepsilon}^{ij} - \frac{1}{3}\delta^{ij}\dot{\varepsilon}^{ij}\right) + S^{ik}\omega^{jk} + \omega^{ik}S^{kj} \tag{20}$$

Where:

$$\dot{\varepsilon}^{ij} = \frac{1}{2}\left(\frac{\partial \mathbf{v}^i}{\partial x^j} + \frac{\partial \mathbf{v}^j}{\partial x^i}\right) \tag{21}$$

And the rotation tensor ω^{ij} is:

$$\omega^{ij} = \frac{1}{2}\left(\frac{\partial \mathbf{v}^i}{\partial x^j} - \frac{\partial \mathbf{v}^j}{\partial x^i}\right) \tag{22}$$

4. SOLUTION ALGORITHM

In this chapter, a fully explicit three-step algorithm is used for both fluid and elastic solid particles which will be explained in details.

4.1. Solution Algorithm for Fluid Particles

In the first step of this algorithm, the momentum equation is solved in the presence of the body forces neglecting all other forces. So, an intermediate velocity is computed as

$$u^* = u_{t-\Delta t} + g_x \Delta t \tag{23}$$

$$v^* = v_{t-\Delta t} + g_y \Delta t \tag{24}$$

As said before, in the second step of fluid flow simulation the temporal velocity is employed to calculate the divergence of viscous stress tensor. Note that the divergence of viscous stress tensor is a vector $\vec{T}$ given by:

$$\left(\frac{1}{\rho}\nabla.\vec{\tau}\right)_i = \vec{T} = T_x \vec{i} + T_y \vec{j} \tag{25}$$

At the end of the second step, the velocity of particle is updated according to

$$u^{**} = u^* + T_x \Delta t = u_{t-\Delta t} + g_x \Delta t + T_x \Delta t \tag{26}$$

$$v^{**} = v^* + T_y \Delta t = v_{t-\Delta t} + g_y \Delta t + T_y \Delta t \tag{27}$$

At this stage particle moved according to temporal velocities (u^{**} , v^{**}) and temporal position of particle is:

$$x^{*} = x_{t-\Delta t} + u^{**}\Delta t \tag{28}$$

$$y^{*} = y_{t-\Delta t} + v^{**}\Delta t \tag{29}$$

Thus far no constraint has been imposed to satisfy the incompressibility of the fluid and it is expected that the density of some particles change during this updating. In fact, with the help of the continuity equation one can calculate the density variations of each particle as

$$\frac{D\rho_i}{Dt} = \sum_j m_j \left(\mathbf{v}_i - \mathbf{v}_j\right).\nabla_i W\left(r_{ij}, h\right) \tag{32}$$

Where ρ_i and $\mathbf{v_i}$ are the density and velocity of particle i. When two particles approach each other, their relative velocity and therefore the gradient of kernel function become negative, so $D\rho_i / Dt$ will be positive and ρ_i will increase. Consequently, this will produce a repulsive force between the approaching particles. In a similar fashion, if two particles are repulsed from each other, an attractive force will be produced to stop this. This interaction based on the relative velocity of particles and the resulting coupling between the pressure and density will enforce incompressibility in the solution procedure.

The velocity field $\hat{\mathbf{v}} = \left(\hat{u}, \hat{v}\right)$ which is needed to restore the density of particles to their original value is now calculated. To do this, in the third step of the algorithm, the momentum equation with the pressure gradient term as a source term is combined with the continuity equation (10) as

$$\frac{1}{\rho_0}\frac{\rho_0 - \rho^{*}}{\Delta t} + \nabla.(\hat{\mathbf{v}}) = 0 \tag{33}$$

$$\hat{\mathbf{v}} = -\left(\frac{1}{\rho^{*}}\nabla P\right)\Delta t \tag{34}$$

to obtain the following pressure Poisson equation

$$\nabla.\left(\frac{1}{\rho^{*}}\nabla P\right) = \frac{\rho_0 - \rho^{*}}{\rho_0\, \Delta t^{2}} \tag{35}$$

Equation (35) can be discretized according to equation (9) to obtain pressure of each particle as

$$P_i = \left(\frac{\rho_0 - \rho_*}{\rho_0 \Delta t^2} + \sum_j \frac{8 m_j}{(\rho_i + \rho_j)^2} \frac{P_j \vec{r}_{ij} . \nabla_i W_{ij}}{\left|\vec{r}_{ij}\right|^2 + \eta^2} \right) \Bigg/ \left(\sum_j \frac{8 m_j}{(\rho_i + \rho_j)^2} \frac{\vec{r}_{ij} . \nabla_i W_{ij}}{\left|\vec{r}_{ij}\right|^2 + \eta^2} \right) \tag{36}$$

using this value for the pressure of each particle one can calculate $\hat{\mathbf{v}}$ according to equation (34) and (7) as

$$\hat{\mathbf{v}}_i = \sum_j m_j \left(\frac{P_i}{\rho_{i\ *}^2} + \frac{P_j}{\rho_j^2} \right) \nabla_i W_{ij} \tag{37}$$

Finally, overall velocity of each particle at the end of time step will be obtained as

$$u_{t+\Delta t} = u^{**} + \hat{u} \tag{38}$$

$$v_{t+\Delta t} = v^{**} + \hat{v} \tag{39}$$

And the final positions of particles are calculated using a central difference scheme in time

$$x_t = x_{t-\Delta t} + \frac{\Delta t}{2} (u_t + u_{t-\Delta t}) \tag{40}$$

$$y_t = y_{t-\Delta t} + \frac{\Delta t}{2} (\mathrm{v}_t + \mathrm{v}_{t-\Delta t}) \tag{41}$$

6. RIGID WALL BOUNDARY CONDITIONS

Boundary conditions always receive special attention in SPH method; here we follow the treatment used by Koshizuka et al. [35] to model the wall boundaries by fixed wall particles, which are spaced according to the initial configuration. Here we employ a kernel with a compact support of $h = 1.5 l_0$, where l_0 is the initial particle spacing. In addition, two lines of dummy particles with properties which are completely similar to boundary particles are also placed outside of solid walls at spacing l_0. The calculation procedure for both wall and dummy particles is completely similar to inner particles, except set the velocity to be zero to represent no-slip boundary conditions.

7. A TEST CASE

A test case that was performed by Hosseini and Amanifard(2007), is presented here to show the capability of the mentioned method, however it is not a test case of the porous media. Using the SPH for porous media is developing and current test case may provide a new idea for such a development.

An Elastic Plate Subjected to Time-Dependent Water Pressure

In this experiment an elastic gate, is clamped at one end and free at the other one, interacts with a mass of water initially confined in a free-surface tank behind the gate.

A schematic view of this 2D problem is shown in figure 2. As it is shown, the left wall consists in an upper rigid part and in a lower deformable plate made of rubber. The rubber plate is free at its lower end, thus representing an elastic gate closing the tank. The geometric dimensions of the system and the physical characteristics of the elastic gate are reported in table 1.

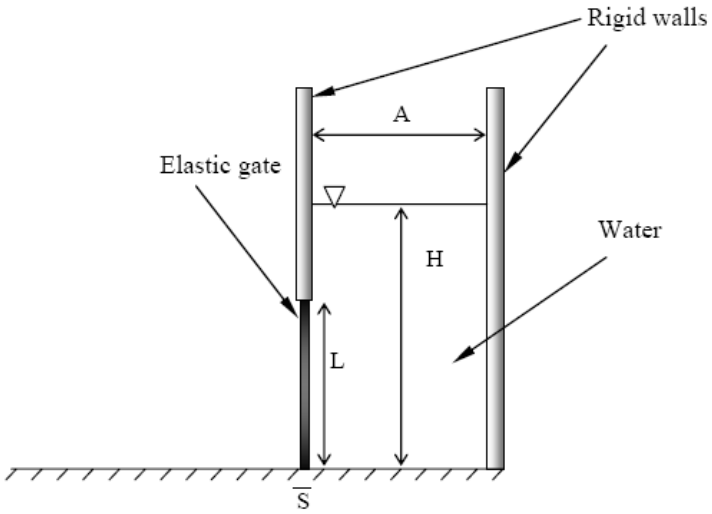

Figure 2. Schematic view of initial configuration.

Table 1. Dimensions of the system and physical characteristics of the rubber plate

Dimensions	
A (m)	0.1
H (m)	0.14
L (m)	0.079
S (m)	0.005
Rubber	
ρ (kg/m^3)	1100
G (N/m^2)	4.27×10^6

In figure 3, the horizontal and vertical displacements computed for the plate (according to presented SPH algorithm and FSI model) are compared with those measured in the digitalized images acquired during the experiments and the results of old SPH model of FSI.

SPH particle positions at six different times are shown in figure 5. These Images are completely in good agreement with the frames from the experiment setup at corresponding times.

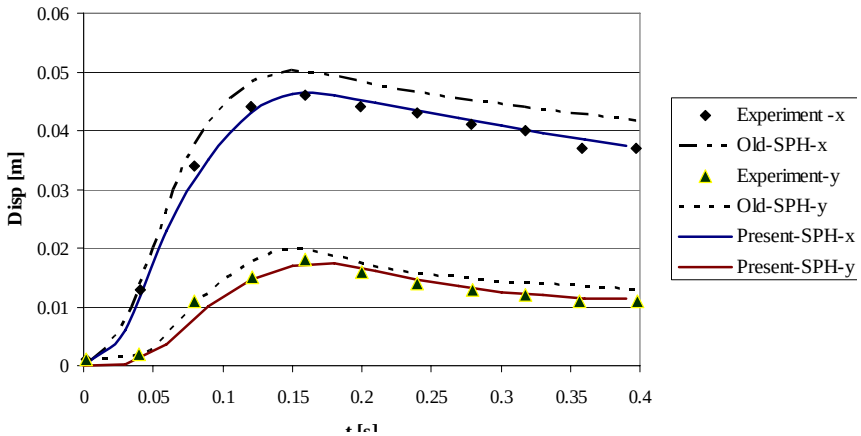

Figure 3. Horizontal and vertical displacements of the free end of the plate.

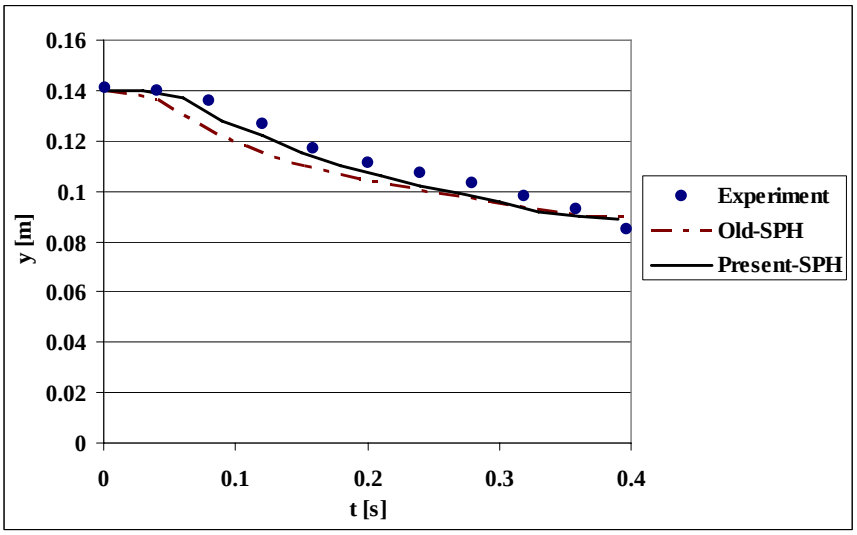

Figure 4. Water level (m) just behind the gate.

The evolution of the free-surface is also well reproduced by the simulation. Figure 5 shows the water level history immediately behind the gate.

CONCLUSION

As it was observed, the accuracy of presented SPH simulation is completely greater than the old one. It is because of using a better algorithm for solid elastic simulation and no special treatment for interface particles (the interface modeled naturally).

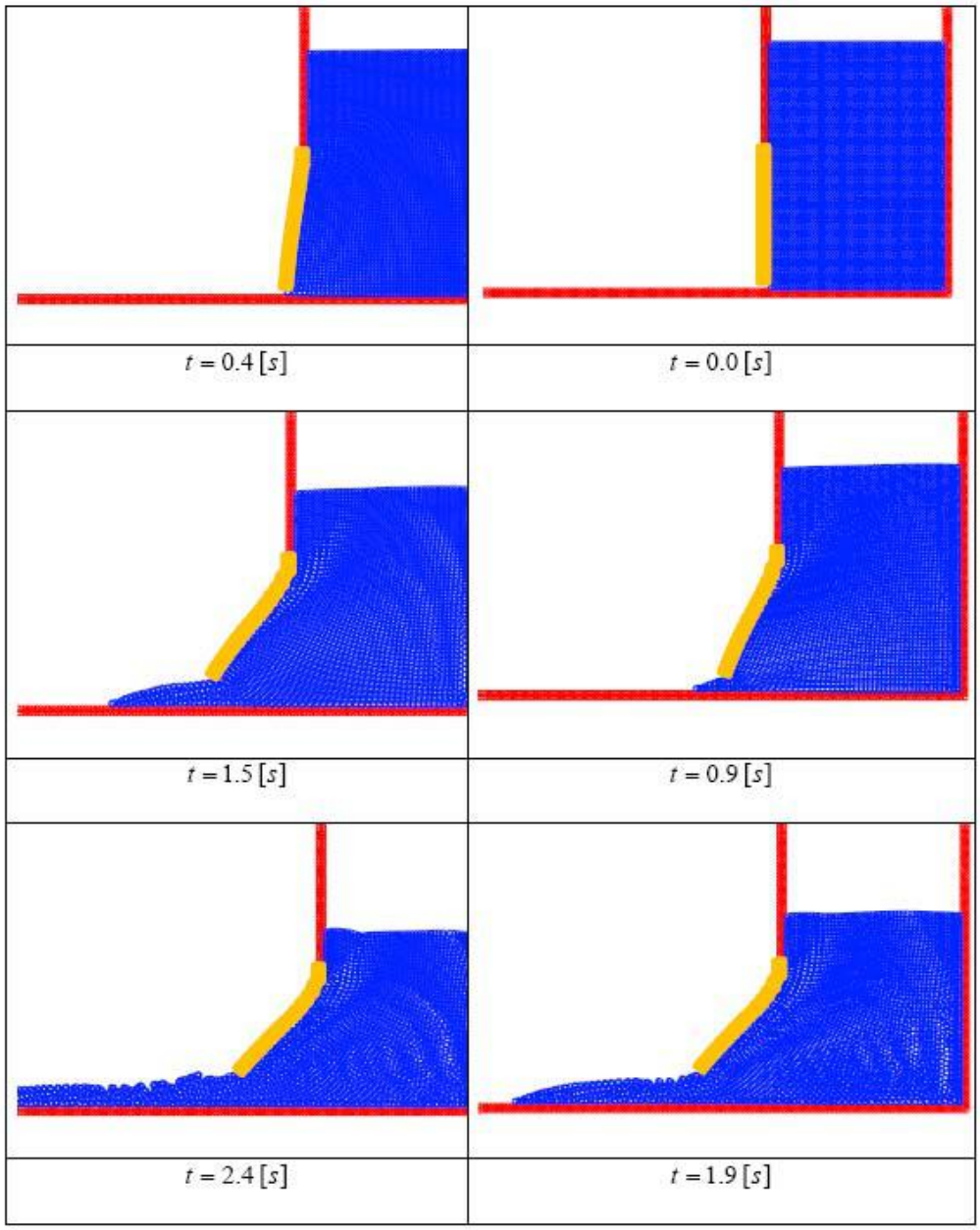

Figure 5. SPH particle positions at six different times.

REFERENCES

[1] Schwartz LM, Martys N, Bentz DP, Garboczi EJ, Torquato S. (1993). Cross-property relations and permeability estimation in model porous media. *Phys. Rev. E.* 48:4584-91.

[2] Snyder LJ, Stewart WE. (1966). Velocity and pressure profiles for Newtonian creeping flow in regular packed beds of spheres. *A. I. Ch. E. Journal ;*12:167-73.

[3] Sorensen JP, Stewart WE. (1974). Computation of forced convection in slow flow through ducts and packed beds Ð II velocity profile in a simple cubic array of spheres. *Chem. Eng. Sci.;*29:8 19-25.

[4] Edwards DA, Shapiro M, Bar-Yoseph P, Shapira M. (1990). The influence of Reynolds-number upon the apparent permeability of spatially periodic arrays of cylinders. *Phys. Fluids*;2:45-53.

[5] Ghaddar CK. (1995). On the permeability of unidirectional fibrous media: a parallel computational approach. *Phys. Fluids* ;7:2563-86.

[6] Meegoda NJ, King IP, Arulanandan K. (1989). An expression for the permeability of anisotropic granular media. *Int. J. Numer Anal. Methods Geomech;*13:575-98.

[7] Larson RE, Higdon JJL. (1986). Microscopic flow near the surface of two-dimensional porous media. Part1. Axial flow. *J. Fluid Mech;*166:449-72.

[8] Larson RE, Higdon JJL. (1987). Microscopic flow near the surface of two-dimensional porous media. Part 2. Transverse flow'. *J. Fluid Mech*;178:119-36.

[9] Qian YH, d'Humires D, Lallemand P. (1992). Lattice BGK models for Navier-Stokes equation. *Europhys Lett;*17:479-84.

[10] Morris JP, Fox PJ, Zhu Y. (1997). Modeling low Reynolds number incompressible flows using SPH. *J. Comput. Phys*;136:214-26.

[11] Zhu Y, Fox PJ, Morris JP. (1997)`Smoothed particle hydrodynamics model for flow through porous media'. In: Proceedings of the 9th International Conference on Computer Methods and Advances in Geomechanics Vol. 2, China, Wuhan, , p. 1041-6.

[12] Zhu Y, Fox PJ, Morris JP. (1999)`A pore-scale numerical model for flow through porous media', *Int. J. Numer Anal Methods Geomech;*23:881-904.

[13] Morris J.P., Zhu Y., Fox P.J. (1999). Parallel simulations of pore-scale flow through porous media, *Comp. Geotech.* 25, 227-246.

[14] Lucy LB. (1977). A numerical approach to the testing of the fission hypothesis. *Astron. J;*83:1013-24.

[15] Gingold RA, Monaghan JJ. (1977). Smoothed particle hydrodynamics: theory and application to non- spherical stars. *Mon. Not. R Astron. Soc*;181:375-89.

[16] Owen JM, Villumsen JV, Shapiro PR, Martel H (1998) Adaptive smoothed particle hydrodynamics methodology ii. *Astrophys. J. Suppl. S.* 116:55–209

[17] Fulbright MS, Benz W (1995) A method of Smoothed Particle Hydrodynamics Using Spheroid Kernels. Astron. J. 440: 254–262

[18] Liu M. B. Liu G. R. (2005). Meshfree particle simulation of micro channel flows with surface tension. *Comput. Mech*.) 35: 332–341

[19] D. Vola and F. Babik and J.C. Latche, on a numerical strategy to compute gravity currents of non-Newtonian fluids, *J. Comp. Physics.* 201(2): 397-420, 2004.

[20] A.K. Chaniotis and D. Poulikakos and P. Koumoutasakos(2002), Remeshed smoothed particle hydrodynamics for the simulation of viscous and heat conducting flows, *J. Comp. Physics*. 182: 67-90.

[21] J. Michael Owen (2002). Remeshed smoothed particle hydrodynamics for the simulation of viscous and heat conducting flows. *J. Comp. Physics.* 182: 67-90.

[22] J.J. Monaghan (1994). Simulating free surface flows with SPH. *J. Comp. Physics.* 110: 399.

[23] H. Takeda and S.M Miyama and M. Sekiya (1994). Numerical Simulation of Viscous Flow by Smoothed Particle Hydrodynamics, *Progress of Theoretical Physics.* 92(5):939-960.

[24] J. P. Gray, J. J. Monaghan, R. P. Swift (2001). SPH elastic dynamics, *Comp. Methods Appl. Mech. Eng.*190:6641-6662.

[25] Carla Antoci , Mario Gallati, Stefano Sibilla (2007). Numerical simulation of fluid–structure interaction by SPH, Computers and Structures.

[26] J.J. Monaghan (1992), Smoothed particle hydrodynamics, *Annul. Rev. Astron. Astrophys.*, 30: 543-574.

[27] M. A. Hosseini and Nima Amanifard (2007). Presenting a New Modified SPH Algorithm for Numerical Fluid-Structure Interaction Studies. Accepted for publication in *Int. J. Eng.*